We have developed a new procedure by which one may measure diffusion constants and spinodal curves in polymer blends. Exponential growth in the concentration gradient $(c - c_0)$ was observed during the early stages of phase separation, after which time the Cahn–Hilliard expression becomes clearly inadequate. From the growth of the scattering intensity and the angular dependence of that scattering, it was possible to give a complete quantitative description of the early stages of polymer blend phase separation in the PS/PVME system.

References and Notes

(1) van Aartsen, J. J. *Eur. Polym. J.* **1970**, *6*, 919.
(2) van Aartsen, J. J. *Eur. Polym. J.* **1970**, *6*, 1105.
(3) Kuwshara, N.; Fenly, D. V.; Tamsky, M.; Chu, B. *J. Chem. Phys.* **1970**, *55*, 1140.
(4) Scholte, Th. G. *Eur. Polym. J.* **1970**, *6*, 1063.
(5) Debye, P. *J. Chem. Phys.* **1959**, *31*, 680.
(6) Goldsbrough, J. *Sci. Prog.* **1972**, *60*, 281.
(7) McMaster, L. P. *Macromolecules* **1973**, *6*, 760.
(8) Koningsveld, R.; Kleintjens, L. A.; Schoffelens, H. M. *Pure Appl. Chem.* **1974**, *39*, 1.
(9) Nishi, T.; Wang, T. T.; Kwei, T. K. *Macromolecules* **1975**, *8*, 227.
(10) Pincus, P. *J. Chem. Phys.* **1981**, *75*, 1996.
(11) de Gennes, P.-G. *J. Chem. Phys.* **1980**, *72*, 4756.
(12) Cahn, J. W. *J. Chem. Phys.* **1965**, *42*, 93.
(13) Hilliard, J. E. In "Phase Transformations". Seminar of the American Society for Metals, Oct 1968, p 497.
(14) Cahn, J. W. *Trans. Am. Inst. Min., Metall. Pet. Eng.* **1968**, *242*, 166.
(15) Langer, J. S. In "Fluctuations, Instabilities and Phase Transitions"; Riste, T., Ed.; Plenum Press: New York, 1975.
(16) Sur, A.; Lebowitz, J. L.; Marro, J.; Kalos, M. H. *Phys. Rev. B.* **1977**, *15*, 3014.
(17) Mruyik, M. R.; Abraham, F. F.; Pound, G. M. *J. Chem. Phys.* **1978**, *69*, 3462.
(18) Varea, C.; Robledo, A. *J. Chem. Phys.* **1981**, *75*, 5080.
(19) Kuwahara, N.; Ishiyawa, M.; Saeki, S.; Kaneka, M. *Rep. Prog. Polym. Phys. Jpn.* **1976**, *13*, 9.
(20) Nishi, T.; Kwei, T. K. *Polymer* **1976**, *16*, 285.
(21) Davis, D. D.; Kwei, T. K. *J. Polym. Sci., Polym. Phys. Ed.* **1980**, *18*, 2337.
(22) Bank, M.; Liffingwell, J.; Thies, C. *J. Polym. Sci., Polym. Phys. Ed.* **1972**, *10*, 1097.
(23) Bank, M.; Leffingwell, J.; Thies, C. *Macromolecules* **1971**, *4*, 43.
(24) Hourston, O. J.; Hughes, I. D. *Polymer* **1978**, *19*, 1181.
(25) Kobertstein, J.; Russell, T. P.; Stein, R. S. *J. Polym. Sci., Polym. Phys. Ed* **1979**, *17*, 1719.
(26) Reich, S.; Cohen, Y. *J. Polym. Sci., Polym. Phys. Ed.* **1981**, *19*, 1255.
(27) Patterson, D.; Robard, A. *Macromolecules*, **1978**, *11*, 690.
(28) Huang, J. S.; Goldberg, W. I.; Bjerkcas, A. W. *Phys. Rev. Lett.* **1974**, *32*, 921.
(29) Bortz, A. B.; Kalos, M. H.; Lebowitz, J. L.; Zendejas, M. A. *Phys. Rev. B* **1974**, *10*, 535.
(30) Sur, A.; Lebowitz, J. L.; Marro, J.; Kalos, M. H. *Phys. Rev. B* **1977**, *15*, 3014.
(31) Marro, J.; Bortz, A. B.; Kalos, M. H.; Lebowitz, J. L. *Phys. Rev. B* **1975**, *12*, 2000.

Melting Behavior of Crystalline/Compatible Polymer Blends: Poly(ε-caprolactone)/Poly(styrene-*co*-acrylonitrile)

Peter B. Rim and James P. Runt*

The Pennsylvania State University, Department of Materials Science and Engineering,
Polymer Science Program, University Park, Pennsylvania 16802.

Received September 29, 1982

ABSTRACT: The crystallinity and melting of compatible poly(ε-caprolactone)/poly(styrene-*co*-acrylonitrile) (PCL/SAN) blends were monitored for samples prepared from both the melt and solution. The development of PCL crystallinity was observed to be dependent on both the blend composition and preparation technique. The glass transition temperature was observed to be a primary cause of the compositional dependence of crystallinity. Solution casting was found to be a technique capable of increasing crystallinity levels for some compositions. The melting behavior of the blends is rather complex. Solution-cast samples exhibited a single endotherm that decreased in temperature with increasing SAN concentration. Both thermodynamic and morphological effects are cited as possible causes of this behavior. Melt-crystallized samples exhibited dual-melting endotherms whose magnitudes vary with blend composition. The melting point of the lower temperature endotherm increased with increasing SAN concentration. A mechanism based on melting, recrystallization, and subsequent remelting is invoked to explain the behavior of the melt-crystallized specimens. Finally, problems encountered when calculating polymer–polymer interaction parameters directly from experimental melting data are discussed.

I. Introduction

Thermal analysis techniques such as differential thermal analysis (DTA) and differential scanning calorimetry (DSC) have been used frequently to study compatible polymer blends. The usefulness of these techniques can be multipurpose. Observation of glass transition temperatures (T_g) that are between those of the pure blend components is often cited as evidence of compatibility. For compatible blends in which one or more of the components are capable of crystallization (crystalline/compatible blends), thermal techniques are often used to monitor crystalline melting points as well as extents of crystallization.

As might be expected, T_g has been observed to be a major factor influencing the degree of crystallinity in crystalline/compatible blends.[1,2] For melt-crystallized specimens crystallization can proceed if the crystallization temperature (T_c) is between the blend equilibrium melting point (T_m°) amd T_g. However, work performed in our laboratory on poly(ε-caprolactone)/poly(styrene-*co*-acrylonitrile) (PCL/SAN) blends has shown that the common blend preparation technique of solution casting can lead to a modification of the temperature range over which crystallization occurs.[1] It was observed that crystallization could be induced in crystalline/compatible blends that are normally amorphous when prepared from the melt. This behavior is believed to result from a solvent-induced crystallization process. This previous study was performed on one composition (80% SAN/20% PCL) of the PCL/SAN blend system. One purpose of the

0024-9297/83/2216-0762$01.50/0 © 1983 American Chemical Society

present work is to extend our studies to include blends encompassing the total compositional spectrum.

For crystalline/compatible systems, melting point (T_m) data are often analyzed by an approach such as that suggested by Nishi and Wang,[3] which yields a value for the polymer–polymer interaction parameter (χ). It is important to be aware that such considerations are only strictly correct when equilibrium melting point values are available. However, in a significant number of studies on the melting of crystalline/compatible blends, nonequilibrium T_m's (i.e., experimentally observed) are used to deduce χ.[2-10] Of major concern is how crystalline microstructure is affected by the addition of a second compatible polymer and/or the mode of sample preparation. In addition, determination of the T_m of the as-formed crystals in a specimen can often be complicated by low polymer thermal conductivity and any annealing that occurs during heating in a DSC or DTA. The results of our study show that extreme care must be taken in attempting to estimate χ from nonequilibrium melting behavior.

II. Experimental Section

The polymers used in this study were a random copolymer of styrene with acrylonitrile (SAN) and poly(ϵ-caprolactone) (Union Carbide Corp., PCL-700). PCL ($T_g \simeq -70$ °C) is a semicrystalline polymer that melts at approximately 60 °C. SAN ($T_g \simeq 100$ °C) is an amorphous polymer that was found by elemental nitrogen analysis to be 76% styrene by weight. The PCL ($M_w = 40\,000$)[11] was kindly provided by Dr. J. V. Koleske of Union Carbide Corp. Seefried and Koleske monitored the change in the glass transition temperature with composition for this blend system and observed intermediate T_g behavior characteristic of a compatible system.[12]

In our study, blends ranging from 90 to 10% SAN by weight and pure samples of PCL and SAN were prepared in both the presence and the absence of solvent. The first step in the solution blending process was to make individual 1% solutions of the respective polymers in tetrahydrofuran (THF) followed by stirring for approximately 4 h. The solutions were subsequently blended in the proper proportions and stirred overnight. Twenty-milliliter aliquots of the resulting solutions were then cast at room temperature into aluminum pans of 57-mm diameter. The resulting films (~35 μm thick) were removed from the pans, placed under vacuum (6×10^{-5} torr) to remove residual solvent, and aged at room temperature for approximately 2 months. Melt crystallization was performed by initially heating the solution-cast blends at 10 °C/min to 360 K in a Perkin-Elmer differential scanning calorimeter (DSC-2). The blends were subsequently quenched in liquid nitrogen and then rapidly warmed to room temperature, where they were also aged for 2 months. Thermal analysis of the blends was performed in the DSC-2 at a heating rate of 10 °C/min unless otherwise noted. Some of the runs were analyzed and recorded with a Perkin-Elmer thermal analysis data station and are noted as such.

All DSC samples were weighed on a Perkin-Elmer AD-2 autobalance. Sample weights varied, depending on the purpose of the experiment. For melting point studies relatively small samples (~0.05–0.4 mg) were analyzed to minimize any complications due to low polymer thermal conductivity.[13,14] Care was also taken to ensure good contact between the sample and the sample pan since this factor has also been shown to influence melting points.[15] Larger samples (~1–7 mg) were used for determination of heats of fusion (ΔH_f) in order to avoid errors inherent in weighing small samples. In addition, the higher range (lower sensitivity) needed to monitor these large samples allowed for more accurate base line construction under melting endotherms. Base lines defining the endothermal areas were drawn according to a method suggested by Gray.[16]

All T_m and ΔH_f data cited are the average of at least two runs. Melting points were determined by superimposing the leading edge of indium on the PCL melting endotherms. T_m was taken as the intersection of the indium leading edge with the constructed base line. Indium was also used to correct these values for the temperature offset of the DSC and as a calibration standard for endothermal areas. Percent crystallinites were calculated assuming a perfect crystalline heat of fusion of 32.4 cal/g for PCL.[17]

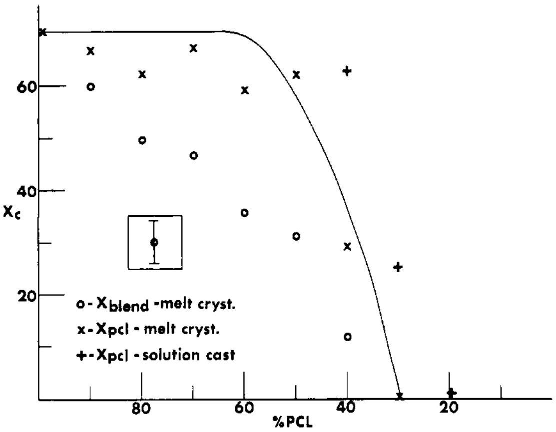

Figure 1. Plot of the predicted and experimental degrees of crystallinity (X_c) vs. composition: (—) predicted PCL crystallinity for melt-crystallized samples assuming that a homogeneous amorphous matrix exists throughout the crystallization process; (○) experimental blend crystallinities for melt-crystallized samples; (×) experimental PCL crystallinities for melt-crystallized samples; (+) experimental PCL crystallinities for solution-cast samples.

III. Results and Discussion

A. Effect of Blend Composition and Preparation Technique. 1. Degree of Crystallinity. Figure 1 shows the effect of blend composition on the percent crystallinity of samples prepared by melt and solution techniques. Considering first the melt-crystallized samples, it was observed that the overall blend crystallinity (○) decreased with increasing SAN content. To ascertain how much of this crystallinity decrease was due to the decrease in the amount of PCL, we calculated the crystallinity of PCL (×) relative to its own weight in the blends. Notice that the normalized degree of crystallinity remains relatively constant with increasing SAN content before dropping sharply in the compositional range of 50–30% PCL. We believe that this behavior is being dictated to a large degree by the variation of T_g with composition. As the SAN content in the blends is increased the blend T_g increases and the tendency for crystallization decreases. This rationale is pleasing when one considers blends at the onset of crystallization; however, of major concern is the nature of the amorphous regions as crystallization proceeds. If during the crystallization of PCL the SAN molecules become trapped within the superstructure of the growing crystals, one might expect a constant amorphous composition at the crystal growth front. Indeed, studies of the spherulitic growth rate in similar systems support this idea.[10,18-22] The extent to which SAN is trapped will depend on the ratio of the crystallization rate to the rate of diffusion of SAN away from the growth front. Note that even a qualitative prediction of this ratio is complex, since both the crystallization and diffusion rates will depend on blend T_g and composition. In addition, the crystallization rate is a function of the supercooling, which will vary upon blending if T_m° changes. Therefore a single model may not accurately describe the crystallization process of all blend compositions.

The most simplistic model which is often used to describe crystalline/compatible blends assumes that the system consists of two phases: a crystalline phase and a homogeneous amorphous phase. We thought that it would be of interest to determine whether such a model is consistent with our data if the restriction of a homogeneous amorphous matrix is imposed throughout the crystallization process. In this model, the composition at the crystal growth front will vary as crystallization proceeds. Considering first blends with compositions of 100 to 50% PCL, we see that the T_g of the amorphous phase (as predicted by the Fox equation[23]) is less than the crystallization temperature (room temperature) from the onset to the conclusion of crystallization even though approximately 70% of the PCL would have been effectively removed from the matrix. This low T_g is consistent with high levels of crystallinity observed for these blends. For PCL concentrations less than 30%, the T_g as monitored by DSC (and as predicted by the Fox equation) is greater than T_c, therefore completely inhibiting crystallization. In the region of intermediate composition, even though the T_g at the onset of crystallization is below T_c, one would expect the cessation of crystallization (if this model is correct) as soon as enough PCL has crystallized such that the T_g of the amorphous region equals T_c. The implication is that one should be able to predict the degree of crystallinity of any melt-crystallized compatible blend from knowledge of only the T_g's of the constituent polymers. The solid line in Figure 1 is the result of calculations performed by assuming that a simple two-phase structure exists during the crystallization process. The Fox equation was used to calculate the percentage of PCL that must phase separate (crystallize) to obtain an amorphous phase composition with $T_g \approx T_c$; the only restriction on these calculations was that PCL could not crystallize to an extent greater than pure PCL. Notice that the calculated curve provides an excellent fit to the experimental data. However, we acknowledge that this simplistic model may not be truly representative of the morphology of the blends during crystallization. Regardless, the good correlation between this model and the experimental data supports the concept that T_g is a primary factor controlling the level of crystallinity in crystalline/compatible blends.

Blends of PCL and SAN were also crystallized at room temperature in the presence of THF. The PCL crystallinities of such solution-cast samples containing 40 and 30% PCL are plotted in Figure 1 (+). Crystallinities determined for all other compositions are identical with those of the melt-crystallized samples within experimental error. Notice that the PCL crystallinities of the solution-cast blends containing 40 and 30% PCL are much larger than those obtained upon crystallization from the melt. This is not surprising when one considers that the crystallization in this system is T_g dependent. We rationalize the observed behavior as follows. At some point in the solvent evaporation process, the polymers precipitate and form a gel containing the constituent polymers as well as solvent. The presence of solvent would cause the gel to possess a T_g lower than would be expected just from consideration of the T_g's of the constituent polymers. At compositions where crystallization is normally limited by the amorphous-phase T_g (i.e., less than ~50% PCL in the PCL/SAN system), the plasticizing action of the solvent may result in greater crystallization. For blends with less than 30% PCL, the THF apparently did not depress the blend T_g's sufficiently for crystallization to occur in the time span of the solvent evaporation. However, one might expect that blends of high SAN content could be crystallized if exposed to a low-T_g environment for a sufficient time period. This idea was investigated in a previous publication.[1] Briefly, we found that it is possible to induce crystallization in SAN-rich blends by controlling a number of sample preparation variables. PCL crystallinities as high as ~65% were obtained for blends composed of only 20% PCL.

B. Melting Behavior. 1. Background. While obtaining the results presented in the previous section, we observed that the melting behavior of the samples was dependent on both the blend composition and preparation technique. To further investigate this behavior we repeated the thermal analysis reported in section A; these studies were performed by employing small sample sizes as described in the Experimental Section. Since the melting behavior of these samples was observed to be rather complex, it is advantageous at this point to review the various factors that can influence melting behavior. With this review as a background, the significance of the ensuing experimental results will become apparent.

In a large number of studies on crystalline/compatible blends the T_m of the crystallizable component has been observed to decrease as the concentration of the noncrystallizable component increases. As will be discussed in a subsequent section, this behavior is characteristic of SAN/PCL blends when prepared from solution. In many cases, this melting point depression phenomenon has been postulated to arise from thermodynamic effects.[2-10] However, there are factors other than polymer–polymer interactions that can influence nonequilibrium T_m's in crystalline/compatible blends. The first question that must be considered is whether the observed melting point represents the T_m of the as-formed crystals. Many semicrystalline polymers have been shown to anneal or reorganize in the DSC or DTA, presumably through a mechanism of partial melting, followed by recrystallization, and then final melting.[13] One would expect that a similar process could occur in semicrystalline blends, thereby making it very difficult to discern the true T_m of the as-formed crystals. Multiple-melting endotherms (usually two) may result from such reorganization processes and, in a few cases, investigators have actually observed a recrystallization exotherm located between two melting peaks in pure semicrystalline polymers.[24,25] For the case of dual-melting behavior, it is sometimes assumed that the low-temperature endotherm reflects the true melting behavior of the as-formed crystals while the higher temperature endotherm represents the melting of material that has undergone annealing upon heating. We will show in a subsequent section that for SAN/PCL blends prepared by cooling from the melt, the actual situation can be far more complicated.

It is also possible to envision a situation where annealing is occurring upon heating but one cannot resolve individual melting peaks. In this case the observed T_m will be a function of the positions and magnitudes of the recrystallization exotherm and the melting endotherms associated with the original crystals and the annealed material. The observed T_m clearly need not be that of the as-formed crystals. Any factor that alters the ability of the original crystals to reorganize will influence the character of the composite melting endotherm and will likely change the observed T_m. This idea is particularly interesting in the case of crystalline/compatible blends if one monitors the melting behavior as a function of blend composition. As an example, consider a blend system containing a crystallizable polymer possessing a relatively low T_g and a high-T_g amorphous polymer. As one increases the amount of the noncrystallizable, high-T_g polymer in the blend, the T_g of the compatible amorphous phase will rise and result in a stiffer matrix surrounding the crystallites. This would tend to inhibit lamellar thickening and result in a decrease in the observed T_m. This effect has been observed and discussed previously for polyethylene[26] and isotactic polystyrene[25] crystals dispersed in matrices of other polymers.

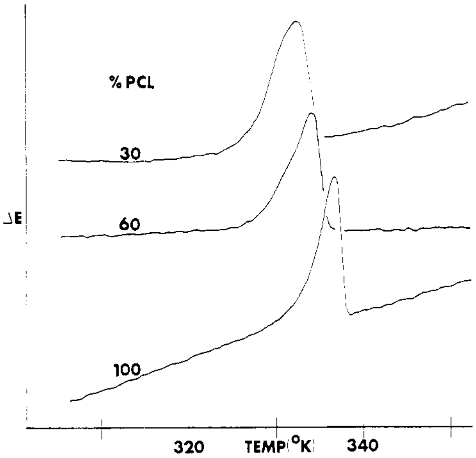

Figure 2. Representative DSC thermograms of solution-cast SAN/PCL blends.

Even in the absence of complications due to reorganizational or matrix effects, other factors can influence T_m. If there is indeed some type of interaction between molecules of the component polymers in a crystalline/compatible blend, one would expect $T_m{}^\circ$ of the crystallizable polymer to be depressed as the concentration of noncrystallizable component increases. If T_c is identical for all compositions, the effective supercooling should decrease as the concentration of the noncrystallizable component increases and one would expect the crystal core thickness (l_c) to increase with increasing concentration of the noncrystallizable component. This behavior has in fact been indicated from small-angle X-ray scattering (SAXS) studies on PCL/poly(vinyl chloride) (PVC) blends, which show a small increase in the PCL crystal thickness with increasing PVC content.[27] This effect alone would result in a T_m increase upon dilution with a second compatible polymer; however, a contrasting effect will be the T_m depression due to interactions between the component polymers. Other complications may arise since $T_m{}^\circ$ (and, therefore, the supercooling) may continually change during an isothermal crystallization process if the composition of the amorphous matrix varies during crystallization. This would result in a distribution of l_c's. The significance of this latter effect is unknown at present because the nature of the amorphous regions in these systems is not well understood.

Finally, it is conceivable that crystallite perfection and lateral crystal size also influence the T_m's in crystalline/compatible blends. One could speculate that the presence of a second compatible polymer would disrupt the packing of the crystalline component, resulting in defective, lower melting crystallites. Spherulitic morphology has been shown to become coarser as the concentration of the noncrystallizable component increases,[28,29] but this does not yield information concerning the perfection of the individual lamellae within the system. Another area of interest is crystallite size. If the lateral dimensions of the lamellae become excessively small (such that side surface free energies become important), melting points could be decreased. However, to our knowledge, this factor has not been explored for crystalline/compatible blends.

2. Solution-Cast Samples. Figure 2 shows representative DSC thermograms of samples prepared by solution casting. Notice that the thermograms exhibit one apparent endotherm, with T_m decreasing with increasing SAN content (the T_m's are graphically represented in Figure 3). As stated previously, similar behavior in other systems has been postulated to arise from polymer–polymer interactions; however, it is important to be aware of the possibility of nonthermodynamic contributions to melting behavior. Both the morphology and annealing behavior of the crystallites could vary upon the addition of a second compatible polymer.

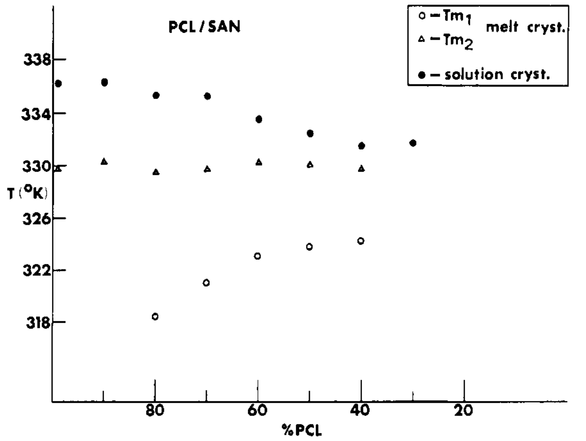

Figure 3. Plot of the melting point vs. composition for solution-cast and melt-crystallized blends. (The error in T_m ($\pm 2\sigma$) is approximately the size of the data points.)

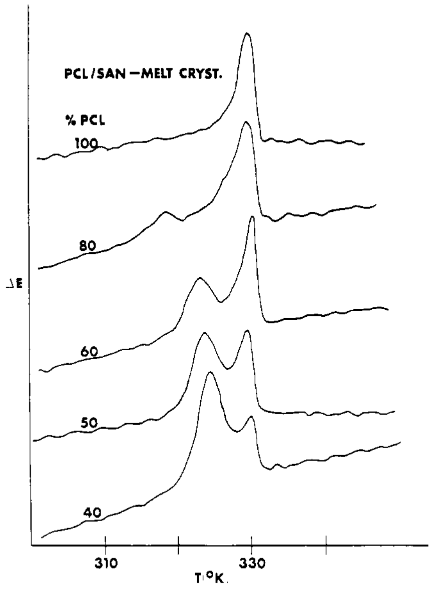

Figure 4. Representative DSC thermograms of melt-crystallized SAN/PCL blends.

Notice that in addition to the melting point changes, the endotherms tend to broaden with increasing SAN content. A variety of possible explanations for this broadening exist. These include heterogeneity of lamellar thickness and crystalline perfection, fluctuations in blend composition, and unresolved multiple-melting endotherms.

3. Melt-Crystallized Samples. In contrast to the solution-cast samples, the DSC thermograms of the melt-crystallized specimens generally exhibit dual-melting endotherms. Figure 4 shows how the character of the multiple-melting endotherms for the melt-crystallized samples varies with composition. With increasing PCL concentration the magnitude of the higher temperature endotherm increases relative to the lower temperature endotherm. This trend continues until 90% PCL, the composition at which the lower temperature endotherm is not observed. In the past, many ideas have been discussed concerning the origin of multiple melting.[13] Of specific interest to us was to determine whether the observed behavior was indicative of the original sample morphology. We therefore performed a heating rate study on a blend of 70% PCL/30% SAN (Figure 5). As the

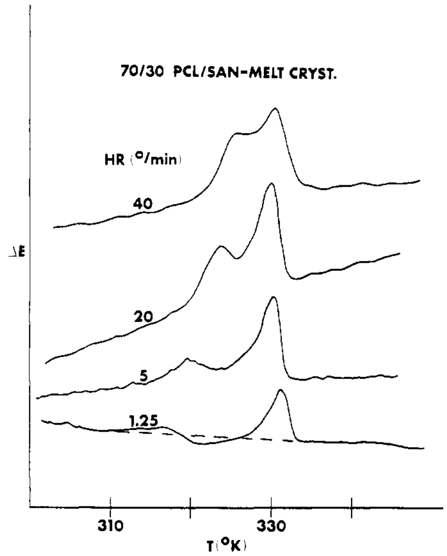

Figure 5. Effect of heating rate on the thermal response of a melt-crystallized SAN/PCL blend (70% PCL).

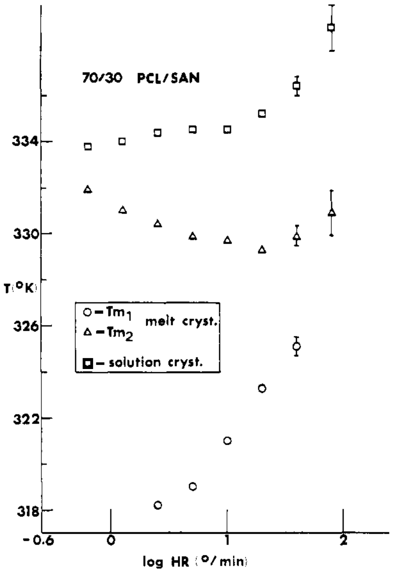

Figure 6. Plot illustrating the effect of heating rate on T_m for solution-cast and melt-crystallized blends. (Unless noted on the figure, the error in T_m ($\pm 2\sigma$) is approximately the size of the data points.)

heating rate is increased from 1.25 to 40 °C/min the magnitude of the lower temperature endotherm increases relative to the higher temperature endotherm. Note the apparent exotherm between the two melting peaks in the sample scanned at 1.25 °C/min. The T_m's also vary with heating rate (Figures 5 and 6). From these observations it is apparent that the melting behavior is being dictated to a large extent by processes occurring during thermal analysis.

The mechanism by which we rationalize the heating rate behavior of the melt-crystallized samples is depicted in Figure 7.[30] We assume that crystalline lamellae are capable of annealing upon heating in the DSC. At slow heating rates, the original crystals are given ample time to reorganize and the melting behavior will contain a relatively large contribution from recrystallization of the original lamellae (C) and melting of the recrystallized material (Mr). The resultant behavior will then be a composite of the peaks due to the melting of the original crystals (M), the recrystallization exotherm, and the melting of the recrystallized material. Note that the resultant curve may bear little resemblance to the melting of the original crystals. As the heating rate is increased, the crystals will have less time to reorganize and C and Mr will decrease in magnitude.

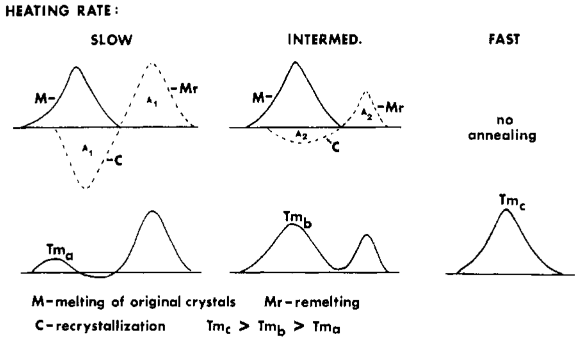

Figure 7. Schematic representation of the melting mechanism proposed to account for for the heating rate dependence of melt-crystallized SAN/PCL blends. The top of the figure shows the melting of the original crystals (M), recrystallization (C), and remelting (Mr). The bottom portion of the figure shows the resultant thermograms that one would expect to observe experimentally. (Note that $T_{m_c} > T_{m_b} > T_{m_a}$).

This mechanism is consistent with the experimental results presented in Figure 5. With increasing heating rate the magnitude of the higher temperature endotherm decreases relative to the lower temperature endotherm because the specimen is given less time to reorganize. The mechanism also correctly predicts the observed T_m behavior (Figure 6). Notice that T_{m_1} (lower T_m) increases dramatically with increasing heating rate. According to the proposed mechanism the position of T_{m_1} is influenced to a large degree by the magnitude of the crystallization exotherm. Since the net effect of the exotherm is to shift T_{m_1} to lower temperatures, one would expect T_{m_1} to occur at lower temperatures for slowly heated samples. The T_m of the higher temperature endotherm is observed to decrease slightly with increasing heating rate before increasing at high heating rates (Figure 6). There are a number of possible explanations for the initial decrease in T_{m_2}. Since the ability to anneal decreases with increasing heating rate, one might expect that the annealed material would be less regular or of a smaller lamellar thickness for samples quickly heated. This would predict a decrease in T_{m_2} with increasing heating rate. For heating rates which exhibit endotherms that overlap it is important to consider how the relative magnitudes of the lower and higher temperature endotherms influence T_{m_2}. Since the ratio of the lower temperature endotherm to the higher temperature endotherm increases with increasing heating rate, one might expect T_{m_2} to be shifted to lower temperatures with increasing heating rate. We believe that the apparent increase in T_{m_2} at high heating rates is the result of thermal conductivity effects. Since polymers typically possess low thermal conductivities, melting points can be significantly increased at high rates because of the time necessary for heat to be transmitted throughout a sample. The possibility of this effect is supported by a heating rate study performed on a solution-cast blend of 70% PCL/30% SAN (Figure 8). The original purpose of the experiment, which will be discussed in detail in a subsequent section, was to determine if the single endotherms that resulted from the solution-cast samples were composed of multiple-melting peaks. Note that the melting points of the solution-cast samples remain relatively constant at slow heating rates before dramatically increasing at heating rates of 40 and 80 °C/min (Figure 6).

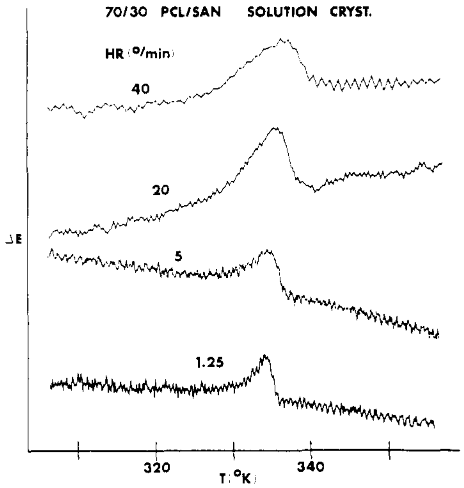

Figure 8. Effect of heating rate on the thermal response of a solution-cast SAN/PCL blend (70% PCL). These thermograms have been monitored on the Perkin-Elmer thermal analysis data station.

With the previously considered melting mechanism as background, we can now discuss the variation of melting behavior with composition for the melt-crystallized samples (Figure 4). Recall that with increasing PCL concentration the magnitude of the higher temperature endotherm increases relative to the lower temperature endotherm. This behavior is consistent with the proposed melting mechanism. One would expect blends of high SAN content to be less capable of annealing because of the rigid nature of the amorphous matrix. This contrasts with blends of high PCL content, which presumably anneal to such a large degree that only the melting of the annealed material is observed. We propose that for samples of high PCL content the lower temperature endotherm is more or less canceled by the crystallization exotherm.

Figures 3 and 4 show that in addition to endothermal size changes with composition, T_{m_1} is also a function of blend composition. Contrary to what would be expected simply from thermodynamic effects, T_{m_1} is observed to increase with increasing SAN content. This behavior is best rationalized by considering how the magnitude of the recrystallization exotherm varies with composition. As the amount of PCL in the blends decreases, the tendency for annealing could decrease, thereby decreasing the size of the recrystallization exotherm. Since the effect of this exotherm is to shift T_{m_1} to lower temperatures, one would expect T_{m_1} to increase with decreasing concentration of PCL. This does not imply that thermodynamic effects are not influencing the T_m's but only that annealing may be masking the thermodynamic depression. It is interesting that the behavior of T_{m_1} correlates with the results of the heating rate study on the melt-crystallized blend of 70% PCL. By either decreasing the concentration of PCL or increasing the heating rate the annealing exotherm would decrease, resulting in an increase of T_{m_1}. However, a similar analogy cannot be drawn for the behavior of T_{m_2}, which decreases somewhat with increasing heating rate but remains relatively constant as the blend composition is varied. The reason for this is unclear at this time.

It might appear that the increase in T_{m_1} with decreasing PCL content could also be explained on the basis of changes in lamellar thickness. Thermodynamic considerations predict that the presence of SAN may decrease the T_m° of PCL. This would result in SAN-rich blends being crystallized at smaller supercoolings than those rich in PCL, assuming all compositions were crystallized at the same temperature. It would therefore be expected that the thickness of the PCL crystallites and, hence, T_{m_1} would increase with increasing SAN concentration. However, recent work suggests that an increase in T_m due to changes in the crystal thickness cannot offset a thermodynamic depression and one would still expect the observed T_m to decrease with increasing concentration of a second compatible component.[31]

It is apparent from the previous discussions that the melting behavior of crystalline/compatible blends can be rather complex. This is especially evident when considering Figure 3, which shows the variation of T_m with composition for blends prepared by both techniques. The possibility of multiple-melting endotherms and variations in annealing behavior and lamellar thickness with blend composition can complicate melting behavior, casting doubt on interaction parameter calculations. In theory one should be capable of increasing the heating rate to the point that no annealing takes place; however, this approach is complicated by low polymer thermal conductivity.

4. Comparison of the Melting Behavior of Melt-Crystallized and Solution-Cast Samples. As discussed in the previous two sections melt-crystallized samples exhibit two melting endotherms whereas solution-cast blends exhibit one apparent melting endotherm. T_m's of samples prepared by both techniques are summarized in Figure 3 for all blend compositions. Notice that for a given composition the endotherm of the solution-cast samples occurs at a higher temperature than either endotherm of the melt-crystallized samples. We believe that this T_m difference may be a reflection of the effective supercooling under which crystallization has occurred. For example, in the case of the solution-cast samples one would expect the solvent to depress the T_m° of PCL during the crystallization process. Therefore, the PCL in the solution-cast samples will crystallize at a lower supercooling than in the melt-crystallized samples. The net result of crystallizing at a lower supercooling would be to increase the lamellar thickness and hence the T_m's of the solution-cast samples relative to the corresponding melt-crystallized samples. Current research is being directed toward monitoring the small-angle X-ray scattering of these samples to test this hypothesis.

The possibility of lamellar thickness differences between samples prepared by the two different techniques can help rationalize why the solution-cast samples exhibit only one endotherm. If the thickness of the PCL crystals in the solution-cast blends is relatively large, one would expect these thicker crystals to be less inclined to reorganize upon heating in the DSC. It is therefore conceivable that the T_m's observed for the solution-cast blends are not influenced by reorganizational processes to the same extent as the melt-crystallized samples. This idea is substantiated by a heating rate study on a solution-cast blend of 70% PCL (Figures 6 and 8). Notice that the melting points remain relatively constant at slow rates before increasing at higher rates. If significant reorganizational processes were occurring, one would expect the T_m to decrease with increasing heating rate. As discussed previously we believe that the large increase in T_m at high heating rates is the result of low polymer thermal conductivity.

IV. Conclusions

1. The crystallinity of melt-crystallized SAN/PCL blends was observed to be dependent on the T_g of the amorphous phase. Essentially, the greater the SAN concentration in the blends, the higher the T_g and the lower the tendency for crystallization. The compositional dependence of crystallinity was modified by crystallizing in the presence of THF. This solution-casting process was

observed to yield samples of higher crystallinity than melt-crystallized samples for certain blend compositions. This behavior is consistent with typical solvent-induced crystallization phenomena. During sample preparation the solvent depresses the T_g of the blend, allowing crystallization to proceed beyond that expected by crystallizing from the melt.

2. The melting behavior of melt-crystallized SAN/PCL blends was observed to be rather complex. Two melting endotherms were observed for compositions of 40–80% PCL. A mechanism in which the original crystals melt, recrystallize, and then remelt is proposed to explain the multiple-melting behavior. This process becomes less prominent with increasing SAN content, presumably due to the increasing matrix T_g. Similar results were not obtained for solution-cast samples, which exhibited only one apparent endotherm.

3. The melting points of samples prepared by the two techniques also varied. The single endotherm of the solution-cast samples was observed at a higher temperature than either endotherm of the melt-crystallized samples for all compositions. The variation of T_m with composition also differed for samples prepared by the two techniques. The T_m's of the solution-cast samples were observed to decrease with increasing SAN content. Both thermodynamic and morphological effects are acknowledged as possible causes of this behavior. The lower temperature endotherm (T_{m_1}) of the melt-crystallized samples increased with increasing SAN content whereas T_{m_2} was found to be independent of the blend composition. This behavior was rationalized by employing the proposed melting mechanism.

4. We conclude that the use of nonequilibrium T_m's to investigate polymer–polymer interactions in crystalline/compatible blends can be complicated by a variety of factors. If these effects are prominent, interaction parameter calculations from melting data will have little or no significance.

Acknowledgment. We thank the National Science Foundation (Grant CPE-8008060) and the Celanese Plastics and Specialties Co. for support of this work. We also thank Dr. Ian R. Harrison for many helpful discussions.

Registry No. Poly(ϵ-caprolactone), 24980-41-4; styrene–acrylonitrile copolymer, 9003-54-7; poly[oxy(1-oxo-1,6-hexanediyl)], 25248-42-4.

References and Notes

(1) Runt, J.; Rim, P. B. *Macromolecules* **1982**, *15*, 1018.
(2) Paul, D. R.; Barlow, J. W.; Bernstein, R. E.; Wahrmund, D. C. *Polym. Eng. Sci.* **1978**, *18*, 1225.
(3) Nishi, T.; Wang, T. T. *Macromolecules* **1975**, *8*, 909.
(4) Aubin, M.; Prud'homme, R. E. *Macromolecules* **1980**, *13*, 365.
(5) Ziska, J. J.; Barlow, J. W.; Paul, D. R. *Polymer* **1981**, *22*, 918.
(6) Roerdink, E.; Challa, G. *Polymer* **1978**, *19*, 173.
(7) Harris, J. E.; Goh, S. H.; Paul, D. R.; Barlow, J. W. *J. Appl. Polym. Sci.* **1982**, *27*, 839.
(8) Kwei, T. K.; Patterson, G. D.; Wang, T. T. *Macromolecules* **1976**, *9*, 780.
(9) Cortazar, M. M.; Calahorra, M. E.; Guzman, G. M. *Eur. Polym. J.* **1982**, *18*, 165.
(10) Martuscelli, E.; Demma, G. B. In "Polymer Blends"; Plenum Press: New York, 1980.
(11) Robeson, M. *J. Appl. Polym. Sci.* **1973**, *17*, 3607.
(12) Seefried, C. G.; Koleske, J. V. *J. Test. Eval.* **1976**, *4*, 220.
(13) Runt, J.; Harrison, I. R. In *Methods Exp. Phys.* **1980**, *16B*, Chapter 9.
(14) Harrison, I. R.; Runt, J. *J. Polym. Sci., Polym. Phys. Ed.* **1979**, *17*, 321.
(15) Harrison, I. R.; Varnell, W. D. *J. Thermal Anal.*, accepted for publication.
(16) Gray, A. P. *Thermochim. Acta* **1970**, *1*, 563.
(17) Crescenzi, V.; Manzini, G.; Calzolari, G.; Borri, C. *Eur. Polym. J.* **1972**, *8*, 449.
(18) Yeh, G. S. Y.; Lambert, S. L. *J. Polym. Sci., Part A-2* **1972**, *10*, 1183.
(19) Wang, T. T.; Nishi, T. *Macromolecules* **1977**, *10*, 421.
(20) Ong, C. J.; Price, F. P. *J. Polym. Sci., Polym. Symp.* **1978**, *No. 63*, 59.
(21) Keith, H. D.; Padden, F. J. *J. Appl. Phys.* **1964**, *35*, 1286.
(22) Berghmans, H.; Overbergh, N. *J. Polym. Sci., Polym. Phys. Ed.* **1977**, *15*, 1757.
(23) Fox, T. G. *Bull. Am. Phys. Soc.* **1956**, *2*, 123.
(24) Mandelkern, L.; Allou, A. L. *J. Polym. Sci., Part B* **1966**, *4*, 453.
(25) Runt, J. *Macromolecules* **1981**, *14*, 420.
(26) Harrison, I. R.; Runt, J. *J. Polym. Sci., Polym. Phys. Ed.* **1980**, *18*, 2257.
(27) Stein, R. S.; Khambatta, F. B.; Warner, F. P.; Russell, T.; Escala, A.; Balizer, E. *J. Polym. Sci., Polym. Symp.* **1978**, *No. 63*, 313.
(28) Keith, H. D.; Padden, F. J. *J. Appl. Phys.* **1964**, *35*, 1270.
(29) Ong, C. J.; Price, F. P. *J. Polym. Sci., Polym. Symp.* **1978**, *No. 63*, 45.
(30) Harrison, I. R.; Landes, B. *J. Macromol. Sci., Phys.*, submitted for publication.
(31) Rim, P. B.; Runt, J. *Macromolecules*, submitted for publication.